Material characterization and fracture prediction with advanced constitutive model and Polar EPS fracture diagram for AA 3104-H19

IOP Conf. Series: Journal of Physics: Conf. Series **1063** (2018) 012156 doi:10.1088/1742-6596/1063/1/012156

Material characterization and fracture prediction with advanced constitutive model and Polar EPS fracture diagram for AA 3104-H19

Robert E Dick[1,*], Yanshan Lou[2], Shunying Zhang[2], Jeong Whan Yoon[2,3,]**

[1]Alcoa Technical Center, 859 White Cloud Road, New Kensington, PA 15068, USA
[2]Institute for Frontier Materials, Deakin University, 75 Pigdons Road, Waurn Ponds, VIC 3216, Australia
[3]Department of Mechanical Engineering, KAIST, 291 Daehak-ro, Yuseong-gu, Daejeon 305-701, Republic of Korea

* robert.dick@alcoa.com / ** j.yoon@deakin.edu.au

Abstract. Material characterizations for plasticity and fracture have been conducted from uniaxial tensile tests, bi-axial bulge test, and disk compression test for a beverage can AA3104-H19 material. The results from the experimental tests are used to determine material coefficients for the Yld2004-18p model [1]. Finite element simulations are developed to evaluate the predicted earing profile. Excellent agreement with the experimental data for eight ears exhibited in AA3014-H19 is achieved using the Yld2004-18p constitutive model. Further mechanical tests are also conducted on the AA3104-H19 to generate fracture data under different stress triaxiality conditions. Tensile tests are performed on the samples with a central hole and notched specimens to achieve tensile and plane-strain conditions. A specially designed torsion test of a double bridge specimen is conducted to generate the points near pure shear conditions. The Nakajima test is also utilized to produce a bi-axial tension condition. The data from the experiments is used to generate the fracture locus in the principal strain space. Mapping from the principal strain space to Polar Effective Plastic Strain (PEPS) space is accomplished for a general yield function. Finite element modeling is used to validate the fracture diagram in the polar space. A hole expansion demonstrates the accuracy of the PEPS fracture theory for the direction for onset of failure.

1. Introduction

The main concept in defining the sheet orthotropic behavior is the yield surface used to describe both the yielding and plastic flow of the material. Because of this dual role of the yield surface, particular care and accuracy for its modeling is required. Also, due to the complexity of the underlying mechanism of plastic flow and the increasingly advanced alloying technologies, yield surface modeling has become more complex, relying on an increasing number of material parameters. Yld2004-18p model [1] utilizes r-value and yield stress data every 15° from the rolling direction as well as a biaxial datum. Thus, based on the combination of these directionalities, Yld2004-18p model is able to predict more than four ears in cup drawing and that a good prediction of these material directionalities controls the overall accuracy of the earing profile as shown in Yoon et al. [2].

Uncoupled ductile fracture criteria were developed based on microscopic mechanisms, various hypotheses or experimental observations of ductile fracture. Brünig et al. [3] developed models for the prediction of ductile fracture based on three distinct fracture mechanisms. Stoughton and Yoon [4] developed an efficient model for the analysis of necking and fracture limits for sheet metals. Mohr and Marcadet [5] proposed the micro-mechanically-motivated Hosford-Coulomb model for predicting of ductile fracture at low stress triaxiality. Lou et al. [6] proposed ductile fracture criterion (DF2016) to describe the fracture behavior of sheet metals from shear to balanced biaxial tension. An enhanced criterion for anisotropic fracture based on linear transformations was also further proposed [7].

Various testing methods for the characterization of the plastic behavior of sheet materials are well established and are used to generate material coefficients for the Yld2004-18p material model. Uniaxial tensile tests, biaxial bulge test, and disk compressions test were utilized to characterize an AA3104-H19 material. Material coefficients are generated using an optimization technique and the plasticity model is verified by comparing experimental and numerical earing profiles resulting from cylindrical cup drawing. For the development of the fracture loci, tensile tests were performed on the samples with a central hole, and notched specimens along 0, 45, and 90 degrees. A specially designed torsion of a double bridge test was also conducted to generate the points near pure shear condition, and the Nakajima test was utilized to produce the bi-axial tension condition. The fracture loci in the principal strain space is generated from the experimental data and it has been mapped to a fracture Polar EPS (Polar Effective Plastic Strain) following Stoughton and Yoon [8]. A numerical simulation of a centralized hole expansion during cylindrical cup drawing with the AA3104-H19 material is performed to compare the failure location with experimental data for the highly anisotropic behavior.

2. Earing prediction with Yld2004-18p function

Uniaxial tensile tests were performed on dogbone shaped specimens using an Instron testing system. The samples were prepared at orientations of 0°, 15°, 30°, 45°, 60°, 75° and 90° from the rolling direction. Also, triplicate hydraulic bulge tests were conducted at standard test conditions (constant true strain rate = 0.005/second and constant true strain rate = 0.060/second with the extensometer oriented at forty-five degrees to the sheet rolling direction) for the AA3104-H19 material. The Barlat Yld2004-18p model is utilized for the prediction of earing during cup drawing. Fig.1 shows the stress and r-value directionalities predicted from Yld2004-18p. The original thickness of the material is 0.274 mm. The reference hardening curve for the rolling direction is $\bar{\sigma} = 331.46 \cdot (0.00018 + \bar{\varepsilon}_p)^{0.05}$. The optimized coefficients are also summarized in Table 1.

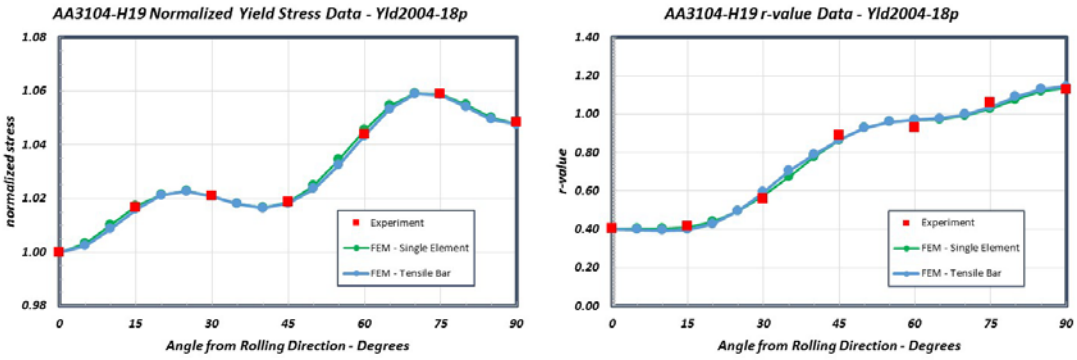

(a) (b)

Figure 1. Anisotropy for AA 3104-H19 : (a) stress ratios (b) r-values

Table1. Material parameters for the Yld2004-18p yield criterion

AA3104-H19	α_1 1.13021	α_2 0.84619	α_3 1.11118	α_4 0.89335	α_5 -0.49552	α_6 0.68614
	α_7 1.47199	α_8 0.96980	α_9 1.22709	α_{10} 0.36757	α_{11} -0.08264	α_{12} 0.52427
	α_{13} 0.68771	α_{14} 1.19374	α_{15} 0.98813	α_{16} 0.42780	α_{17} 0.99205	α_{18} 0.63589

The numerical simulation of the cup drawing process is performed with User defined MATerial model (UMAT) linked with LS-DYNA. The detailed cup geometry is shown in Dick and Yoon [9]. The deformable sheet, or blank, is modeled using 13680 shell elements (type=16) with full iterative plasticity. The element uses the Bathe-Dvorkin transverse shear treatment to eliminate w-mode hourglassing. Other modes of hourglassing are eliminated in the shell by virtue of the selective reduced (S/R) integration. The friction coefficient between sheet and tools is assumed to be constant and taken as μ=0.03. The blank-holder force of 8.9 kN is applied through the use of non-linear springs attached from a rigid plate to the lower pressure pad. The non-linear springs is a modeling technique to allow for a robust application of the pressure pad force and prevents unconstrained rigid body motions. The Yld2004-18p model shows excellent agreement with the experimental data in both the earing amplitude and earing profile as displayed in Fig. 9. Observations show even the small ears around 0° and 180° are successfully predicted.

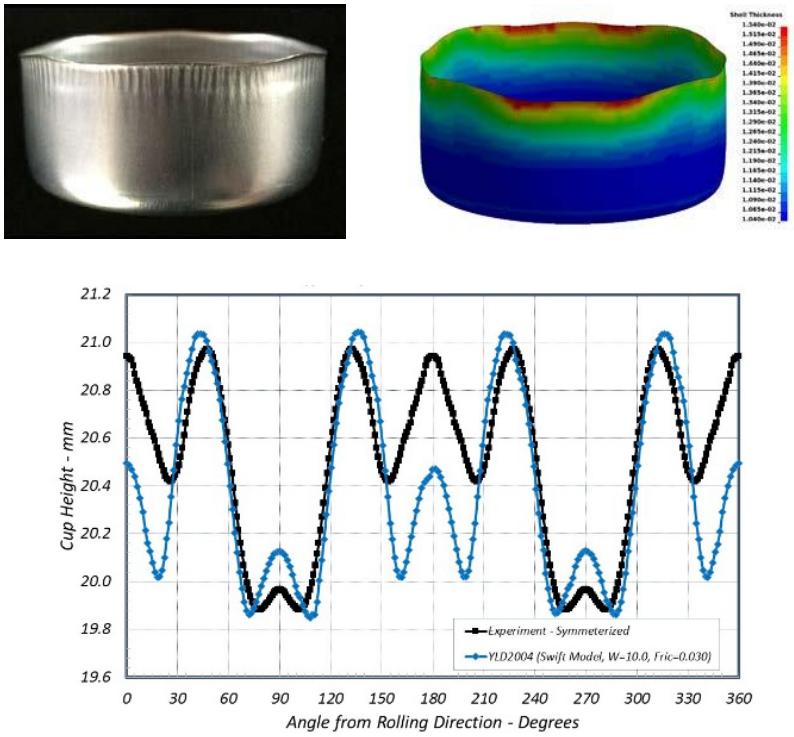

Figure 2. Earing profile obtained from a cup drawing test

3. Fracture modeling with Polar EPS fracture criterion

For the development of the fracture loci, tensile tests were performed on the samples with a central hole, and notched specimens along 0, 45, and 90 degrees. The purpose of the tests is to represent uniaxial tension and plane-strain triaxiality conditions. A specially designed torsion of a double bridge test was also conducted to generate the points near pure shear condition, and the Nakajima test was utilized to produce the bi-axial tension condition. A DIC method is used to characterize fracture strains under various triaxialities. Table 2 and Figure 3 show the von Mises equivalent strains near fracture for various testing.

Table 2. Summary of AA3104-H19 fracture tests.

Test	Hole	Notched	Double Bridge	Nakajima
Fracture Strain	0.1545	0.0997	0.3036	0.2751

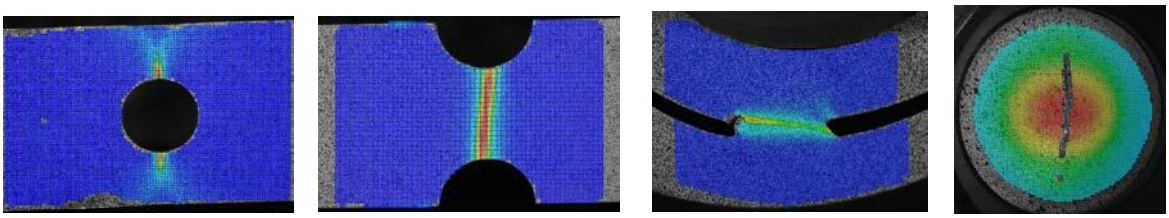

(a) (b) (c) (d)

Figure 3. The von Mises equivalent strains: (a) uniaxial, (b) plane strain, (c) shear, (d) biaxial

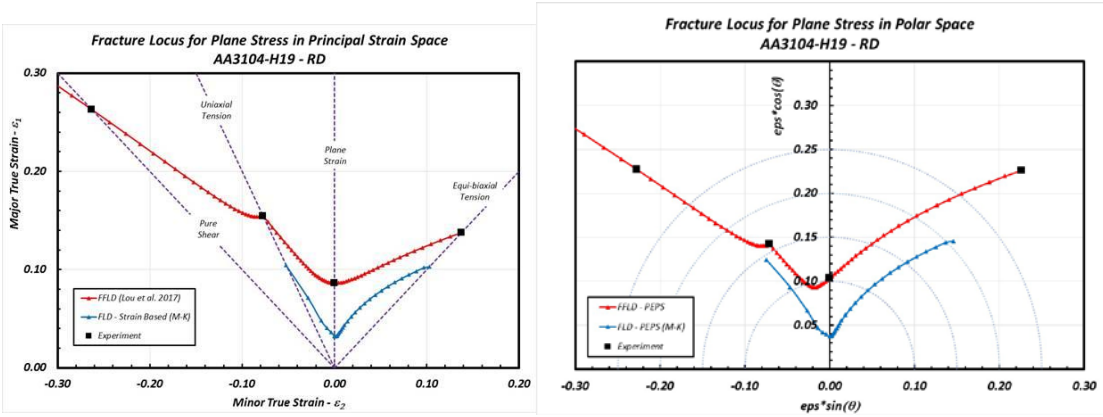

(a) (b)

Figure 4. Forming limit and fracture Loci : (a) Principal strain space (b) Polar EPS space

The fracture loci in the principal strain space is generated at Figure 4(a) from the experimental data. In the figure, the fracture locus of AA3104-H19 is constructed by a ductile fracture criterion [6], i.e.,

$$\left(\frac{2}{\sqrt{L^2+3}}\right)^{C_1}\left(\left\langle\frac{f(\eta,L,C)}{f(1/3,-1,C)}\right\rangle\right)^{C_2}\bar{\varepsilon}_f^p = C_3 \quad \text{where} \quad f(\eta,L,C) = \eta + C_4\frac{(3-L)}{3\sqrt{L^2+3}} + C \tag{1}$$

The values generated from the test data are C_1 = 2.1593, C_2 = 5.2987, C_3 = 0.1545, C_4 = 1.9205, C = 1.3598. The necking limit (forming limit) curve predicted from M-K model is also displayed to show the difference between necking and fracture. A large portion of post-necking strain exists.

Stoughton and Yoon [8] proposed a polar EPS forming limit diagram for nonlinear strain paths. It can be extended to the Polar EPS forming and fracture diagram as shown in Figure 4(b). The mapping procedure from strain-based fracture limit to Polar EPS fracture limit is the same as the one for forming limit mapping procedure shown in Stoughton and Yoon [8] for Hill's (1948) yield function. The mapping procedure has been generalized for a general (non-quadratic) yield function with nonlinear strain paths in Dick and Yoon [9].

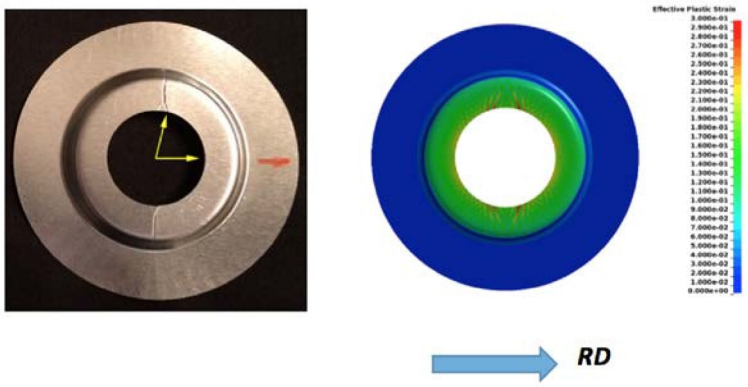

Figure 5. Failures in experiment and simulation for hole expansion process

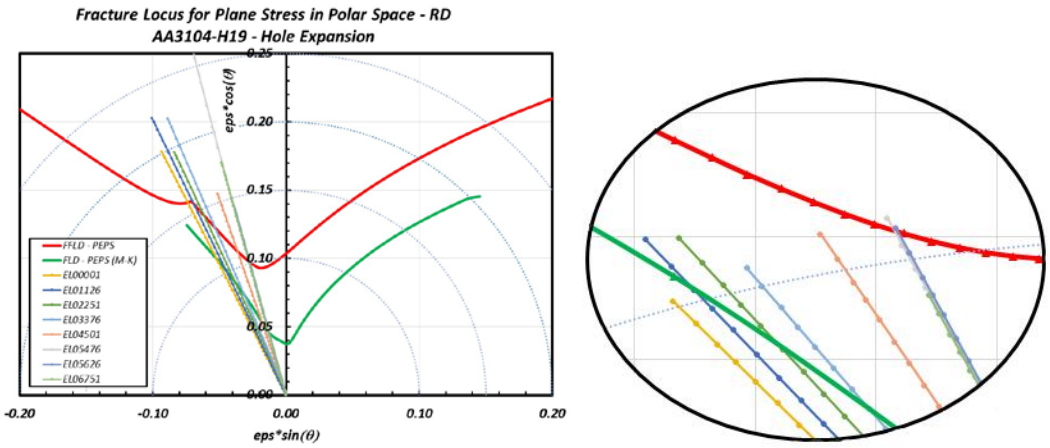

Figure 6. (a) Fracture prediction with Polar EPS at the final stage (b) Detailed view at the onset of fracture.

The experimental drawing of an AA3104-H19 circular blank with a centralized hole is carried out at room temperature in a hydraulic press with maximum capacity of 5 tons. The associated tooling dimensions are given in Dick and Yoon [9]. The circular blank has a diameter of 76.124 mm and a centralized hole with a diameter of 22.860 mm. The drawing process is performed with a constant punch travel speed of 140 mm/s and a constant blank-holder force of 8.9 kN. All forming tools are made of AISI A2 steel with 58 – 60 Rockwell C hardness having a surface roughness of about 2-4 μ m (finished working surfaces). A controlled amount of oil lubricant is applied to both sides of the blank to reduce the frictional forces between the forming tools and the blank sheet during the experiments.

The draw depth of the blank is adjusted using stop blocks and shims to control the overall depth and to capture the onset of fracture. Figure 5 shows the onset of fracture at 75° from the rolling direction. In Figure 6(a) the Polar EPS diagram shows the loading for various directions. A detailed view of one sample showing the fracture initiation is provided in Figure 6(b). The results show that failure initiates with element ID 5476 at 74° from the rolling direction (experimentally 75° from the rolling direction). The strain path is quite linear up to the point of failure as shown in the graph. The difference in the draw-depth between experiment and simulation is 3.93%. The discrepancy in the draw depth may come from sensitive lifting (warping) of thin sheet metal.

4. Conclusions

In this paper, material characterization data was generated for an AA3104-H19 beverage can bodystock alloy using an advanced visual 3D Aramis system. Excellent agreement was achieved between the experimental and numerical directional r-values and stress ratios used in the Barlat Yld2004-18p model. The complex experimental earing profile was accurately predicted using the material coefficients generated. The fracture locus in the principal strain space was developed using tensile tests, a double bridge torsion test, and the Nakajima test. A generalized mapping technique was utilized to map from principal strain space to stress triaxiality space, principal stress space, and PEPS space. A model of a hole expansion during cup drawing demonstrated the robustness of the PEPS fracture theory for the condition of a highly anisotropic material and accurately predicts the onset and location of failure.

References

[1] Barlat F, Aretz H, Yoon J W, Karabin M E, Brem J C, Dick R E 2005 *Int. J. Plast*icity **21** 1009.
[2] Yoon J W, Barlat F, Dick R E, Karabin M E 2006 *Int. J. Plasticity* **22** 174.
[3] Brünig M., Chyra O., Albrecht D., Driemeier L., Alves M 2008 *Int. J. of Plasticity* **24** 1731.
[4] Stoughton T B, Yoon J W 2011 *Int. J. Plasticity* **27** 440.
[5] Mohr D, Marcadet S J 2015 *Int. J. Solids Struct* **67**/**68** 45.
[6] Lou Y, Chen L, Clausmeyer T, Tekkaya A E, Yoon J W 2017 *Int. J. Solids Struct.* **112** 169.
[7] Lou Y, Yoon J W 2018 *Int. J. Plasticity* **101** 125.
[8] Stoughton T B, Yoon J W 2012 *Int. J. of Solids Struct* **49** 3616.
[9] Dick R E, Yoon J W 2018 *Int. J. Solids Struct* (on line).